# Transferable Tight-Binding Potential for Hydrocarbons

Yang Wang and C.H. Mak
Department of Chemistry, University of Southern California, Los Angeles, CA 90089–0482
(Revision 2.0: October 29, 2018)

A transferable tight-binding potential has been constructed for heteroatomic systems containing carbon and hydrogen. The electronic degree of freedom is treated explicitly in this potential using a small set of transferable parameters which has been fitted to small hydrocarbons and radicals. Transferability to other higher hydrocarbons were tested by comparison with *ab initio* calculations and experimental data. The potential can correctly reproduce changes in the electronic configuration as a function of the local bonding geometry around each carbon atom. This type of potential is well suited for computer simulations of covalently bonded systems in both gas-phase and condensed-phase systems.

### I. INTRODUCTION

Computer simulation has become an important theoretical tool in our understanding of complex molecular systems. The two simulation techniques in statistical mechanics – molecular dynamics and Monte Carlo – commonly used to explore the microscopic origin of macroscopic behaviors of many-body systems require as their input realistic microscopic interactions between the constituents. In this paper, we describe a general approach for constructing transferable potentials for heteroatomic systems based on tight-binding Hamiltonians. A potential for systems containing carbon and hydrogen is reported here. It is part of an ongoing project to construct potentials for reactive systems of interest to organic chemistry, biochemistry and materials research.

Systems containing carbon and hydrogen atoms having strong covalent bonds are interesting because of their central role in organic chemistry. Carbon atoms can assume three different hybridizations – sp,  $sp^2$  and  $sp^3$  – depending on the local and global chemical environment, and because of this carbon forms single, double, triple and conjugated bonds in compounds of many different geometries with tetrahedral, planar, linear, ring and cage structures. To understand these systems using computer simulations, it is necessary to first develop an interaction potential for carbon–hydrogen systems which could account for the complexities of the carbon–carbon and carbon–hydrogen covalent bonds.

Pairwise potentials cannot describe covalently bonded hydrocarbons. A recent effort to construct potentials that can describe reactions in covalently bonded systems was first made by Tersoff [1] who used an empirical bondorder type potential to describe primarily silicon–silicon and other covalent bonds. This method was later extended to hydrocarbons by Brenner [2] who used a set of complex functional forms to parametrize the variation of the bonding geometry on each carbon atom based on its first and second nearest–neighbor carbon and hydrogen atoms. The resulting potential involves a large set of parameters.

In another recent approach, a potential based on the tight-binding Hamiltonian has been used to describe covalent bonding in homoatomic systems containing either carbon or silicon [3–9], as well as adsorbed hydrogen on silicon surfaces [10–12]. This approach treats the electronic degrees of freedom explicitly using a small set of transferable parameters. Chemical bonding results from filling the single-particle orbitals obtained from the diagonalization of the tight-binding Hamiltonian. This alternative approach to constructing interatomic potentials has many advantages over conventional parametrization schemes. First, because of its quantum mechanical origin, this potential has the requisite functional form that is able to describe bond breakage and bond formation. Second, only a small set of parameters is necessary to parametrize a large class of molecular interactions. Third, the potential is highly transferable, i.e. the parametrization is obtained by fitting to only a very small set of chemical species (typically four or five), but the potential is extendible to very large systems that may be substantially more complex.

In this letter, we report a new transferable minimum-basis tight-binding (TB) potential for hydrocarbons. We believe this is one of the first successful applications of the tight-binding potential to describe covalent bonding and chemical reactions in heteroatomic systems. Our results on hydrocarbons indicate that using this approach we are able to generate potential energy surfaces which compare well with high-level *ab initio* calculations. This potential is well suited for dynamical simulations because of its simplicity and its ability to account for a large variety of bonding configurations.

## II. METHOD

Hydrocarbons have strong covalent two-centered directional bonds. To describe the hybridization and the directional bonding character in hydrocarbons, we adopt

a semi-empirical minimum basis tight-binding Hamiltonian. The tight-binding Hamiltonian, which considers only the 2s and 2p valence electrons of carbon and the 1s electron in hydrogen, is given by

$$H_{\rm TB} = \sum_{\alpha,i} \epsilon_{\alpha}^{i} a_{\alpha,i}^{+} a_{\alpha,i} + \sum_{\alpha,\beta,i,j} t_{\alpha,\beta}^{ij}(r_{ij}) a_{\alpha,i}^{+} a_{\beta,j} \qquad (1)$$

where i and j label the atoms and  $\alpha$  and  $\beta$  label the atomic orbitals.  $\epsilon_{\alpha}^{i}$  is the atomic orbital energy of atom i and orbital  $\alpha$ .  $t_{\alpha,\beta}^{ij}$  is the hopping matrix element between atomic orbital  $\alpha$  on atom i and  $\beta$  on atom j. Eq. (1) is the conventional tight-binding Hamiltonian often used for solids [4].

In our system, there are four types of hopping matrix elements between carbon atoms:  $t_{ss\sigma}^{\rm CC}$ ,  $t_{sp\sigma}^{\rm CC}$ ,  $t_{pp\sigma}^{\rm CC}$ ,  $t_{pp\pi}^{\rm CC}$ , and two types of hopping matrix elements between carbon and hydrogen:  $t_{ss\sigma}^{\rm HC}$ ,  $t_{sp\sigma}^{\rm HC}$ . The detailed forms of the hopping matrix elements will be discussed later. Note that since there is no electron–electron interactions in Eq. (1),  $H_{\rm TB}$  can be exactly diagonalized as a noninteracting system, yielding the molecular orbitals. The electronic configuration is then defined by putting the requisite number of electrons into the one-electron orbitals subject to the exclusion principle.

The cohesive energy of the system is defined as

$$E_{\text{coh}} = E_{\text{val}} + \sum_{i < j} E_{\text{core}}^{ij}(r_{ij}) - \sum_{i} E_{\text{atom}}^{i}, \qquad (2)$$

where  $E_{\text{val}}$  gives the total energy due to the valence electrons, the core repulsion energy  $E_{\text{core}}^{ij}$  comes from the screened ion-ion interactions between atoms i and j, and the atomic energy  $E_{\text{atom}}^{i}$  is the reference energy of the isolated atom i in the dissociation limit.

The valence energy  $E_{\rm val}$  comes from two terms:

$$E_{\text{val}} = \sum_{\gamma} n_{\gamma} \epsilon_{\gamma} + \sum_{\gamma} U \delta_{n_{\gamma}, 2}$$
 (3)

The first contribution to  $E_{\rm val}$  comes from the molecular orbital energies, summed over all orbitals resulting from diagonalizing the tight-binding Hamiltonian.  $n_{\gamma}$  is the occupation number of orbital  $\gamma$ , and  $\epsilon_{\gamma}$  is the single particle energy of orbital  $\gamma$ . In other words, the first term in Eq. (3) is simply the contribution of  $H_{TB}$  to the total energy. The second term in Eq. (3) places a restriction on the electrons occupying the same molecular orbitals. This U-term describes empirically the extra Coulomb repulsion and correlation energy that arise when two electrons are in the same molecular orbital  $\gamma$ . This term contributes only when the molecular orbital is fully occupied, i. e., the occupational number  $n_{\gamma}$  is 2. It is similar in spirit to the U-term in the Hubbard model [13] and is included in an attempt to describe electron correlation in an approximate way. Because of the *U*-term  $(U \ge 0)$ , an energy penalty is paid each time a pair of electrons (of different spins) go into the same orbital. Therefore it is possible in some circumstances that total energy is made more favorable by exciting an electron from a doubly occupied level to an unoccupied orbital higher in energy to avoid paying the penalty. Consequently, the valence energy  $E_{\rm val}$  has to be minimized with respect to the occupation numbers  $\{n_\gamma\}$ .

For the tight-binding Hamiltonian, we use the Slater–Koster parameterization scheme [14] for the electronic hopping matrix elements. We adopt scaling forms [6] for the distance dependence of the hopping matrix elements as well as for the core repulsive interactions,

$$t_{\alpha,\beta}(r) = t_{\alpha,\beta}(r_0) \left(\frac{r_0}{r}\right)^{n_a} \exp\left[-n_b \left(\frac{r}{r_t}\right)^{n_c} + n_b \left(\frac{r_0}{r_t}\right)^{n_c}\right]$$
(4)

$$E_{\text{core}}(r) = E_{\text{core}}(r_0) \left(\frac{r_0}{r}\right)^{m_a} \exp\left[-m_b \left(\frac{r}{r_c}\right)^{m_c} + m_b \left(\frac{r_0}{r_c}\right)^{m_c}\right]$$
(5)

where  $r_t$  and  $r_c$  are cutoff distances for the hopping matrix elements and repulsive interactions, and the coefficients and power exponents  $n_a$ ,  $n_b$ ,  $n_c$ , and  $m_a$ ,  $m_b$ ,  $m_c$  determine the general shape and sharpness of the cutoff functions. For the same pair of atoms, the reference bond distance  $r_0$  is the same for both the hopping matrix element and the core repulsion. Unlike the original formulation [6], however, we do not demand the hopping parameters to have the same power exponent  $n_c$  as the core repulsion  $m_c$ .

The tight-binding Hamiltonian explicitly considers the contribution of the electrons to the total energy of the system. It is a natural extension of the often used extended Hückel model in organic chemistry [15]. In strongly covalently bonded systems, the molecular orbitals are localized and the chemical bonds are directional. Consequently, the overlap of the wavefunctions are mainly along the line connecting two atoms, and two-center integrals dominate the electron-electron interactions, while three-center and four-center integrals are negligible. By parameterization of the hopping matrix elements, we have taken into account the two-center interactions. Correlation effects, which are very important in certain circumstances, are completely missing in the conventional molecular orbital theory. Some correlation effects have been reintroduced into our potential via the Hubbard-like U-term in the Hamiltonian. Although the U-term seems to have been implemented in an ad hoc manner, it plays a central role in determine the occupation of the molecular orbitals. In particular, it guarantees that molecules dissociate correctly without anomalous charges in the separated atom limit. For example, a CH radical in the tight-binding Hamiltonian without Uwill dissociate to give the unphysical products  $H^- + C^+$ . In addition to producing the total energy of the system, the tight-binding Hamiltonian also generates the single particle energy states. These single-electron energies are

useful for an approximate picture of the electronic density of states.

There are two parts to the potential: the carbon-hydrogen interactions and the carbon-carbon interactions. We will briefly describe how the parameters of these two parts of the potential were obtained.

#### A. Carbon-Hydrogen Interactions

For the carbon–hydrogen interactions, the hopping matrix elements and repulsion parameters at the reference bond distance  $r_0$ ,  $t_{ss\sigma}^{\rm HC}(r_0)$ ,  $t_{sp\sigma}^{\rm HC}(r_0)$ , and  $E_{\rm core}^{\rm HC}(r_0)$  were first fitted to the experimental energies for CH, CH<sub>2</sub>, CH<sub>3</sub> and CH<sub>4</sub>, taken from Ref. [16]. Since the C–H bondlengths in these four CH species are similar, we set the reference bond distance to  $r_0 = 1.09$ Å. Care was taken to ensure that the resulting hopping matrix elements would reproduce a planar equilibrium structure for CH<sub>3</sub>. Then the power exponents  $n_a$  for the hopping matrix elements, the power exponent  $m_a$  for the core repulsion and the cutoff functions were chosen to give the correct experimental equilibrium bond distance of CH<sub>4</sub> as well as the correct breathing mode frequency of CH<sub>4</sub>. The resulting parameters are listed in Table I.

### **B.** Carbon-Carbon Interactions

There are currently available several sets of carboncarbon tight-binding parameters [7,8,17]. For this work, we have developed a new set. For the carbon-carbon interactions, the four hopping matrix elements  $t_{ss\sigma}^{\rm CC}(r_0)$ ,  $t_{sp\sigma}^{\rm CC}(r_0)$ ,  $t_{pp\sigma}^{\rm CC}(r_0)$ , and  $t_{pp\pi}^{\rm CC}(r_0)$ , and the repulsion parameter  $E_{\rm core}^{\rm CC}(r_0)$  were fitted to the carbon–carbon bond energies of  $C_2$ ,  $C_2H_2$ ,  $C_2H_4$ , and  $C_2H_6$  at  $r_0 = 1.312\text{Å}$ . The bond energies of C<sub>2</sub> and C<sub>2</sub>H<sub>4</sub> were taken from experiments [16,18], whereas the bond energies of C<sub>2</sub>H<sub>2</sub> and  $C_2H_6$  at  $r_0 = 1.312$ Å were deduced from the respective bond dissociation energies at their equilibrium distances and the corresponding force constants of the carbon-carbon bonds. Then the power exponents for the hopping matrix elements, the power exponents for the core repulsion and the cutoff functions were fitted to the equilibrium carbon-carbon bondlengths and force constants in C<sub>2</sub>, C<sub>2</sub>H<sub>2</sub>, C<sub>2</sub>H<sub>4</sub>, and C<sub>2</sub>H<sub>6</sub>. The resulting carbon-carbon interaction parameters are listed in Table I.

## III. RESULTS

In this section, we will analyze specific features of our tight-binding (TB) hydrocarbon potential. A comparison of the TB potential to *ab initio* calculations and experimental data is summarized in Tables II to VI.

TABLE I. Parameters for the tight-binding potential.

	arameters for the tight-binding potential.
$\epsilon_s^{ ext{C}}$ $\epsilon_p^{ ext{C}}$ $\epsilon_s^{ ext{H}}$	-10.290 eV
$\epsilon_{p}^{\mathrm{C}}$	$0.0~{ m eV}$
$\epsilon_{\rm s}^{\rm H}$	$-0.50~\mathrm{eV}$
Ű	$3.0\mathrm{eV}$
$\overline{r_0^{ ext{CH}}}$	1.09 Å
$t_{ss\sigma}^{ m CH}(r_0)$	-6.9986  eV
$t_{sp\sigma}^{\mathrm{CH}}(r_0)$	$7.390   \mathrm{eV}$
$E_{core}^{\mathrm{CH}}(r_0)$	$10.8647~\mathrm{eV}$
$n_a^{\text{CH}}$ for $t_{ss\sigma}^{\text{CC}}$	1.970
$n_a^{\text{CH}}$ for $t_{sp\sigma}^{\text{CC}}$	1.603
$m_a^{\text{CH}}$	3.100
$r_t^{ ext{CH}}$	$2.0~{ m \AA}$
$n_c^{\text{CH}}$	9.0
$n_b^{\rm CH}$ for $t_{ss\sigma}^{\rm CH}$	1.970
$n_b^{\rm CH}$ for $t_{sp\sigma}^{\rm CH}$	1.603
$r_c^{ m CH}$	$1.90~{ m \AA}$
$m_c^{\rm CH}$	10.0
$m_b^{ m CH}$	3.100
$r^{CC}$	1.312 Å
$t_{ss\sigma}^{\rm CC}(r_0)$ $t_{sp\sigma}^{\rm CC}(r_0)$ $t_{pp\sigma}^{\rm CC}(r_0)$ $t_{pp\sigma}^{\rm CC}(r_0)$ $t_{pp\sigma}^{\rm CC}(r_0)$ $t_{p\sigma}^{\rm CC}(r_0)$	$-8.42256  \mathrm{eV}$
$t_{sp\sigma}^{\rm CC}(r_0)$	$8.08162~\mathrm{eV}$
$t_{pp\sigma}^{\text{CC}}(r_0)$	$7.75792~\mathrm{eV}$
$t_{pp\pi}^{CC}(r_0)$	-3.67510  eV
$E_{core}^{\mathrm{CC}}(r_0)$	22.68939  eV
$n_a$ for $t_{ss\sigma}$	1.29827
$n_a^{\rm CC}$ for $t_{sp\sigma}^{\rm CC}$	0.99055
$n_a^{\rm CC}$ for $t_{pp\sigma}^{\rm CC}$	1.01545
$n_a^{\rm CC}$ for $t_{nn\pi}^{\rm CC}$	1.82460
$m_a^{\rm CC}$	2.72405
$r_t^{\mathrm{CC}}$	$2.00~{ m \AA}$
$n_c^{\rm CC}$ for $t_{ss\sigma}^{\rm CC}$ , $t_{sp}^{\rm CC}$	$c_{pp\sigma}^{C}$ , $t_{pp\sigma}^{CC}$ , and $t_{pp\pi}^{CC}$ 5.0 $c_{p\sigma}^{CC}$ , $t_{pp\sigma}^{CC}$ , and $t_{pp\pi}^{CC}$ 1.0
$n_b^{\rm CC}$ for $t_{ss\sigma}^{\rm CC}$ , $t_{sp}^{\rm CC}$	$t_{pp\sigma}^{\text{C}}, t_{pp\sigma}^{\text{CC}}, \text{ and } t_{pp\pi}^{\text{CC}}$ 1.0
$r_c^{\text{CC}}$	1.9 Å
$m_c^{\rm CC}$	7.0
$m_b^{\rm CC}$	1.0

## A. Structures

In Table II, the equilibrium geometries of small hydrocarbons from the TB potential are compared to ab initio calculations [16,18] and experimental results [19]. Excellent agreement with the experimental values was found. For the species with only carbon–hydrogen interactions, i.e. CH<sub>4</sub> and CH<sub>3</sub>, our semiempirical potential reproduces the correct equilibrium geometries and the correct carbon–hydrogen bondlengths to within 0.01 Å. For the molecules involving not only carbon–hydrogen interaction but also carbon–carbon interactions, i.e. C<sub>2</sub>H<sub>2</sub>, C<sub>2</sub>H<sub>4</sub>, C<sub>2</sub>H<sub>6</sub>, C<sub>6</sub>H<sub>6</sub>, excellent agreement with experimental results is also achieved. The carbon–hydrogen bonds in these four hydrocarbons are only slightly longer compared to experimental data and the experimental trend that the carbon–hydrogen bondlength increases from

TABLE II.	Tight-binding,	ab initio and ex	perimental	equilibrium	geometries fo	r simple hydrocar	bons. All ab init	tio results
are derived fr	om calculations	using a 6-31G**	basis set u	inless otherw	ise indicated.	All bondlengthes	are in Å.	

Molecule	Point group	Feature	ТВ	HFa	MP4	Expt. <sup>b</sup>
CH <sub>3</sub>	$D_{3h}$	r(C–H)	1.079	1.075	1.078	1.079
$CH_4$	$T_d$	r(C-H)	1.094	1.084	1.094	1.094
$C_2H_2$	$D_{\infty h}$	r(C-H)	1.066	1.057	1.06	1.058
(triple)		r(C-C)	1.183	1.186	1.22	1.208
$C_2H_4$	$D_{2h}$	r(C-H)	1.094	1.076	1.08	1.0836
(double)		r(C-C)	1.341	1.316	1.34	1.337
		∠CCH	$122.8^{\circ}$	$121.75^{\circ}$	$121.5^{\circ}$	$121.25^{\circ}$
$C_2H_6$	$D_{3d}$	r(C-H)	1.104	1.086	1.09	1.091
(single)		r(C-C)	1.546	1.527	1.53	1.536
		∠CCH	$110.8^{\circ}$	$111.2^{\circ}$	$111.0^{\circ}$	$110.90^{\circ}$
$C_6H_6$	$D_{6h}$	r(C-H)	1.095	$1.08^{\rm c}$	$1.09^{c}$	1.084
(conjugated)		r(C-C)	1.428	$1.38^{\rm c}$	$1.39^{c}$	1.397

<sup>&</sup>lt;sup>a</sup> Refs. [16] and [18].

sp to  $sp^3$  hybridization is nicely reproduced. Our TB potential also reproduces correctly the trend that the carbon–carbon bondlength decreases from  $C_2H_6$  to  $C_2H_6$  in the order single > conjugated > double > triple bonds. The carbon–carbon bondlengths in single and double bonds are within 0.01Å from the experimental values, while conjugated and triple CC bonds are within 0.03Å from the experimental data. The bond angles are also in excellent agreement with experimental measurements.

## B. Vibrational Frequencies

Next we examine the properties of the potential energy surface away from the minimum. In Table III, the vibrational frequencies are tabulated and compared to experimental and *ab initio* results [18,19]. Note that the fitting of the parameters involves only the C-H and C-C stretching mode frequencies, while all other frequencies are derived from the TB potential, and they reproduced the vibrational spectra remarkably well. Strong anharmonic effects are observed in small hydrocarbons, and thes have been well established theoretically [20] and experimentally [21].

The vibrational frequencies for CH<sub>3</sub> and CH<sub>4</sub> are all within 5% of the MP2 calculations except for the deformation mode in CH<sub>4</sub> which is within 10%. The slightly larger apparent disagreement with the experimental data on the umbrella mode of the CH<sub>3</sub> is due to strong anharmonic effects. Figure 1 shows the TB potential energy as a function of the C–H bondlength for CH<sub>4</sub> constrained in the tetrahedral geometry. Clearly, the TB predictions agree well with MP4 results even for large deviations from the equilibrium structure.

In the case of  $C_2H_2$ , the CC stretching frequency is 7% larger than the MP2 result. Other high energy CH modes are in excellent agreement—with the MP2 results. The

two low-energy bending modes seem stiffer in our empirical potential than the MP2 results, but the discrepancy with experimental data can be largely attributed to anharmonicity. In the case of  $C_2H_4$ , all modes agrees well with the MP2 results, even the low energy ones. The CC stretching frequency is correct to within 3% compared to the experimental value. In the case of  $C_2H_6$ , in general all modes agrees well with the MP2 results. The CC stretch mode is 10% higher than MP2. The most noticeable discrepancy is the zero frequency predicted by the TB potential for the torsional motion because there is no barrier for the torsional motion in the TB potential for C<sub>2</sub>H<sub>6</sub>. This lack of a torsional barrier is a direct consequence of the symmetry of  $C_2H_6$  within the minimum-basis TB Hamiltonian. The energy barrier in the torsional motion arises from the steric interaction between the third nearest-neighbor hydrogens and this component is currently unaccounted for by the present model.

# C. Energetics

In chemical reactions, bonds are broken and new ones are reformed. The reaction energy will depend crucially on the energetics of different species involved in the reaction. In Table IV and V, TB predictions of the energetics involving the breakage of carbon-hydrogen and carbon-carbon bonds under different situations are compared to ab initio calculations and experimental data In Table IV, the energetics of the sequential removal of hydrogen atoms from methane are summarized. When each hydrogen is being removed, the remaining carbon-hydrogen bonds are allowed to relax to the minimum energy configuration. During the bond breaking process, we start from a stable closed-Removal of one hydrogen proshell species  $CH_4$ . duces a planar CH<sub>3</sub> radical with one unpaired electron.

<sup>&</sup>lt;sup>b</sup> Ref. [19].

<sup>&</sup>lt;sup>c</sup> 3-21G.

TABLE III. Vibrational frequencies (in  $cm^{-1}$ ) for methane (CH<sub>4</sub>), the methyl radical (CH<sub>3</sub>), acetylene (C<sub>2</sub>H<sub>2</sub>), ethylene (C<sub>2</sub>H<sub>4</sub>), and ethane (C<sub>2</sub>H<sub>6</sub>),

Molecule	Symmetry	Description	ТВ	$\mathrm{MP2^{a}}$	Expt. <sup>b</sup>
$\mathrm{CH}_4$	$a_1$	s-stretch	3162	3115	2917
	e	d-deform	1690	1649	1534
	$t_2$	d-stretch	3252	3257	3019
		d-deform	1570	1418	1306
$CH_3$	$a_1$	s-stretch	3207	3208	3004
	$a_2$	umbrella mode	411	404	606
	e	d-stretch	3419	3398	3160
		scissor	1552	1478	1288
$C_2H_2$	$\sigma_g^+$	CH stretch	3546	3593	3374
		CC stretch	2146	2006	1974
		CH stretch	3355	3516	3289
	$\pi_g$	CH bend	811	444	612
	$\pi_u$	CH bend	897	783	730
$C_2H_4$	$a_{1g}$	CH <sub>2</sub> s-stretch	3272	3231	3026
		CC stretch	1680	1724	1623
		$CH_2$ scissor	1561	1425	1342
	$a_u$	CH <sub>2</sub> twist	1158	1083	1023
	$b_{1g}$	$\mathrm{CH}_2$ a-stretch	3305	3297	3103
		$\mathrm{CH}_2$ rock	1398	1265	1236
	$b_{1u}$	$CH_2$ wag	1102	980	949
	$b_{2g}$	$CH_2$ wag	1084	931	943
	$b_{2u}$	CH <sub>2</sub> a-stretch	3344	3323	3106
		$\mathrm{CH}_2$ rock	899	873	826
	$b_{3u}$	$\mathrm{CH}_2$ s-stretch	3221	3222	2989
		$CH_2$ scissor	1651	1523	1444
$C_2H_6$	$a_{1g}$	CH <sub>3</sub> s-stretch	3113	3086	2954
		$\mathrm{CH}_3$ s-deform	1633	1493	1388
		CC stretch	1157	1040	995
	$a_{1u}$	torsion	0	452	289
	$a_{2u}$	$CH_3$ s-stretch	3148	3104	2986
		$\mathrm{CH}_3$ s-deform	1614	1494	1379
	$e_g$	$\mathrm{CH}_3$ d-stretch	3168	3228	2969
		$\mathrm{CH}_3$ d-deform	1639	1520	1468
		$\mathrm{CH}_3$ rock	1336	1264	1190
	$e_u$	$\mathrm{CH}_3$ d-stretch	3201	3215	2985
		$\mathrm{CH}_3$ d-deform	1621	1604	1469
		$\mathrm{CH}_3$ rock	911	783	822

<sup>&</sup>lt;sup>a</sup> 6-31G\* MP2 calculations from [18].

TABLE IV. Calculated and experimental bond energies (in kcal) for sequential removals of hydrogen from methane.

. ,	=		=	
Theory	$\mathrm{CH}_4$	$\mathrm{CH}_3$	$\mathrm{CH}_2$	СН
TB	107	119	106	85
$\mathrm{HF^{a}}$	87	88	101	55
$MP2^{a}$	109	110	109	73
$MP4^{a}$	110	112	107	76
Expt. <sup>b</sup>	112	116	107	84

 $<sup>^{\</sup>rm a}$  6-31G\*\* calculations from Refs. [16] and [18]

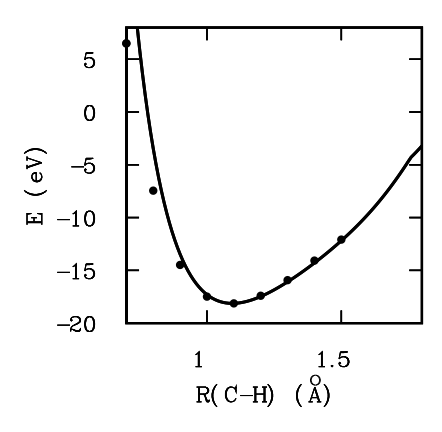


FIG. 1. The cohesive energy of methane as a function of the carbon–hydrogen bondlength (constrained to maintain its  $T_d$  symmetry): from MP4 6-31G\*\* (circles), from TB (solid line). The MP4 results are shifted to the experimental cohesive energy.

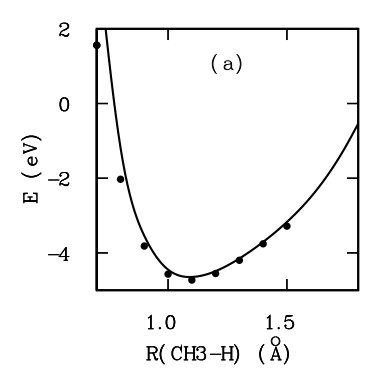
Removal of another hydrogen atom from CH<sub>3</sub> produces a bent CH<sub>2</sub> with two unpaired electrons. Finally, the removal of a third hydrogen produces CH with three unpaired electrons. The sequence of products obtained under sequential removal of hydrogen from CH<sub>4</sub> involves a number of very different hybridizations, and hence the resulting electronic configurations and geometries are rather diverse. Table IV shows that our semi-empirical TB potential can reproduce the energetics quite satisfactorily. The errors in the sequential carbon–hydrogen dissociation energies are within 5 kcal from the experimental data, and the results are much better than *ab initio* Hartree-Fock calculations. The order of the carbon–hydrogen bond strengths is also correctly reproduced.

The carbon–carbon bond dissociation energies in  $C_2H_6$ ,  $C_2H_4$  and  $C_2H_2$  are shown in Table V. In the case of  $C_2H_6$ , a single carbon–carbon bond is broken and the system dissociates from a closed-shell structure into two open-shell methyl radicals. The double bond in  $C_2H_4$  is harder to break than the single bond and the end product is two open shell  $CH_2$  species. The triple bond in  $C_2H_2$  contains the most energy among the three. Our empirical potential reproduces the three different bond energies excellently.

The diversity of organic compounds relies on the ability of carbon atoms to assume different hybridizations in order to form single, double and triple bonds. During chemical reactions, carbon atoms will rehybridize from one configuration to another continuously. A successful potential should be able to describe such processes closely. It will therefore be a more stringent test for our TB potential to see if it will reproduce the correct rehybridization behavior along the reaction path.

<sup>&</sup>lt;sup>b</sup>References [18] and [19].

<sup>&</sup>lt;sup>b</sup> Ref. [16]



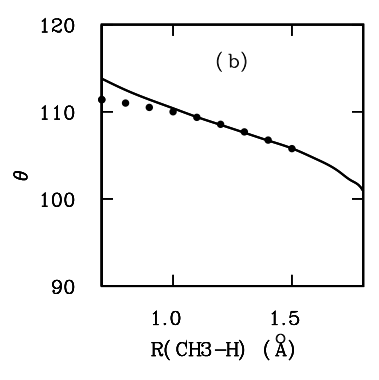


FIG. 2. The calculated (a) cohesive energy and (b) HCH<sub>3</sub> angle change due to the variation in the hybridization by gradually pulling one hydrogen atom out from methane: from MP4 6-31G\*\* (circles), from TB (solid line).

In Fig. 2(a), we show the potential energy curve for the removal of one hydrogen from the tetrahedral  $\mathrm{CH_4}$  to yield a planar  $\mathrm{CH_3}$ . In the process of pulling one hydrogen out of the tetrahedron, the carbon atom reconfigures itself from  $sp^3$  to  $sp^2$  accordingly to open up the umbrella formed by the other three hydrogen atoms until a planar geometry is attained. In Figure 2(b), the HCH<sub>3</sub> angle is plotted as a function of the H–CH<sub>3</sub> distance during the rehybridization of the carbon atom. The predictions of the TB potential agree well with *ab initio* MP4 calculations.

## D. Transferability

By far, the most significant feature of the TB potential is its high degree of transferability. The TB potential has been fitted only to small molecules and radicals. In this section, we will demonstrate the transferability of the TB potential by comparing the TB predictions to experimental results for very much larger system.

Extended structures can be produced by carbon-carbon bonds. One important example is the cage structure of  $C_{60}$ . There are 12 pentagons and 20 hexagons in  $C_{60}$  and all 60 atoms are equivalent.

TABLE V. Calculated and experimental carbon–carbon bond energies (in kcal) for single, double and triple bonds.

	$\mathrm{H_{3}C-CH_{3}}$	$H_2C = CH_2$	$HC \equiv CH$
ТВ	94	177	235
$\mathrm{HF}^{\mathrm{a}}$	69	119	167
$MP2^{a}$	100	177	246
$MP4^{a}$	98	177	236
Expt. <sup>b</sup>	97	179	236

<sup>&</sup>lt;sup>a</sup> 6-31G\*\*.

TABLE VI. Comparison of tight-binding predictions for atomization energies (in eV) of straight-chain alkanes.

n	Experimental <sup>a</sup>	ТВ
1	18.22	18.13
2	30.90	31.03
3	$43.3^{\rm b}$	43.90
4	$56.2^{\mathrm{b}}$	56.78
5	$69.0^{\mathrm{b}}$	69.65
6	$81.8^{\rm b}$	82.52

<sup>&</sup>lt;sup>a</sup>Ref. [25].

Because of the spherical cage structure, carbon atoms do not have either pure  $sp^3$  or  $sp^2$  bonding. The chemical bonds in the pentagons, which are often called "single bonds", are 0.04 Å longer than the remaining "double bonds" in the hexagons. This difference between the double and single bond distances is very nicely reproduced by the TB potential, although the absolute value predicted by the TB potential for a single bond is 0.05 Å too long. The TB potential also predicts an atomization energy of 7.12 eV per carbon atom, which compares very favorably with the experimental result of 7.02 eV per carbon atom [22,23].

Another example of an extended structure produced by carbon-carbon bonds is the sheet structure of graphite. The experimental atomization energy of graphite is 7.37 eV per carbon atom [24]. Ignoring interplanar interactions, our TB potential predicts 7.40 eV per carbon atom.

The benzene molecule which has conjugated CC bonds also presents an interesting test for the TB potential. The experimental atomization energy is 59.56 eV while the TB potential predicts 59.72 eV. This yields a C–C bond energy of 145 kcal, which is between the CC single and double bond energies given in Table II.

For the first six straight-chain alkanes  $C_nH_{2n+2}$ , we have listed the TB predictions for the atomization energy in Table VI. The agreement with experimental values is almost quantitative. The TB potential predicts an average increment of 12.9 eV per additional  $CH_2$  unit, which is very close to the experimental value 12.8 eV.

Finally, we examine one cyclic alkane. The lowest en-

<sup>&</sup>lt;sup>b</sup> Refs. [16] and [18].

<sup>&</sup>lt;sup>b</sup>Estimates corrected for zero-point energies.

ergy conformation of cyclohexane is the chair form. Experimentally, the chair form is more stable than the boat form by 5.5 kcal. This difference between the chair and the boat forms is due to steric hindrance which as discussed above is unaccounted for by the current model. Therefore, in the present form, the TB potential predicts essentially no energy difference between them. The barrier between these two states is predicted to be about 4.8 kcal/mol (with the transition state assumed to be the totally relaxed planar structure). Experimentally, this barrier is about 10.8 kcal/mol.

#### IV. CONCLUSION

We have described a transferable semi-empirical minimum basis tight-binding Hamiltonian for treating reactions involving hydrocarbons. This potential treats the electronic degrees of freedom explicitly, describing the interatomic interactions using a small set of transferable parameters. Chemical bonding results from the diagonalization of the tight-binding Hamiltonian and then the filling of the one-particle energy levels with electrons. This approach can be systematically extended to include more elements across the periodic table. Our results on hydrocarbons show that the electronic configuration depends sensitively on the local bonding configurations around each atom. The rehybridization of a carbon atom from  $sp^3$  to  $sp^2$  under a change of geometry from a tetrahedral CH<sub>4</sub> to a planar CH<sub>3</sub> radical can be followed closely and agrees well with high level ab initio calculations. The energetics and topologies of all carbon-carbon bonds – single, double, triple and conjugated bonds — can be reproduced accurately. Transferability to substantially larger systems have been demonstrated. Due to its simplicity and its ability to describe a large variety of bonding topologies, our approach will be useful for dynamical simulations of reactive systems in both the gas phase and the condensed phase.

#### ACKNOWLEDGMENTS

This research is sponsored by the Army Research Office under the ARO–URI program, Grant Number DAAL03-92-G-0175. We thank Lance Braswell for his assistance during this project.

- J. Tersoff, Phys. Rev. Lett. **56** (1986) 632;
   Phys. Rev. Lett. **61** (1988) 2879; Phys. Rev. B. **38** (1989) 9902; Phys. Rev. B. **39** (1989) 5566; Phys. Rev. Lett. **64** (1990) 1757.
- [2] D. W. Brenner, Phys. Rev. B 42 (1990) 9458.

- [3] D. J. Chadi, Phys. Rev. Lett. 41 (1978) 1062;
   Phys. Rev. Lett. 43 (1979) 43; Phys. Rev. Lett. 59 (1988) 1691.
- [4] W. A. Harrison, Electronic Structure and the Properties of Solids: the Physics of the Chemical Bond, (Freeman, San Francisco, 1980).
- [5] D. Tománek and M. A. Schlüter, Phys. Rev. Lett. 56 (1986) 1055; Phys. Rev. B. 36 (1987) 1208.
- [6] L. Goodwin, A. J. Skinner, and D. G. Pettifor, Europhys. Lett. 9 (1989) 701.
- [7] C. H. Xu, C. Z. Wang, C. T. Chan, and K. M. Ho, J. Phys.: Cond. Matt. 4 (1992) 6047.
- [8] D. Tománek and M. A. Schlüter, Phys. Rev. Lett. 67 (1991) 2331; G. F. Bertsch, A. Bulgac, D. Tománek, and Y. Wang, Phys. Rev. Lett. 67 (1991) 2690; Yang Wang, George F. Bertsch, and David Tománek, Z. Phys. D 25 (1993) 181.
- [9] C. Z. Wang, K. M. Ho, and C. T. Chan, Phys. Rev. B 45 (1992) 12227; Phys. Rev. Lett. 70 (1993) 611; C. Z. Wang and K. M. Ho, Phys. Rev. Lett. 71 (1993) 1184.
- [10] K. C. Pandey, Phys. Rev. B **14** (1976) 1557.
- [11] D. C. Allan and E. J. Mele, Phys. Rev. Lett. **53** (1984) 826; Phys. Rev. B **31** (1985) 5565.
- [12] B. J. Min, Y. H. Lee, C. Z. Wang, C. T. Chan, and K. M. Ho, Phys. Rev. B 45 (1992) 6839; Phys. Rev. B 46 (1992) 9677.
- [13] J. Hubbard, Proc. R. Soc. London Ser. A 276 (1963) 238.
- [14] J.C. Slater and G.F. Koster, Phys. Rev. **94** (1954) 1498.
- [15] R. Hoffmann, J. Chem. Phys. 39 (1963) 1397; A. B. Anderson, J. Chem. Phys. 62 (1975) 1187.
- [16] E. A. Carter and W. A. Goddard III, J. Chem. Phys. 88 (1988) 3132.
- [17] L. Goodwin, J. Phys. Condens. Matter 3, (1991) 3869.
- [18] W. J. Hehre, L. Radom, P. Schleyer, and J. A. Pople, Ab Initio Molecular Orbital Theory, (John Wiley & Sons, New York, 1986).
- [19] G. Herzberg, Molecular Spectra and Molecular Structure III. Electronic Spectra and Electronic Structure of Polyatomic Molecules, (Krieger Publishing Company, Malabar, Florida, 1991).
- [20] G. T. Surratt and W. A. Goddard III, Chem. Phys. 23 (1977) 39.
- [21] C. Yamada, E. Hirota, and K. Kawaguchi, J. Chem. Phys. **75** (1981) 5256.
- [22] W. V. Steele, R. D. Chirico, N. K. Smith, W. E. Billups, P. R. Elmore, and A. E. Wheeler, J. Phys. Chem. 96 (1992) 4731.
- [23] The quoted experimental value is determined using an estimate for the zero-point energy based on an average vibration frequency of 700 cm<sup>-1</sup>.
- [24] C. Kittel, Introduction to Solid State Physics, 6th edition, (John Wiley & Sons, New York, 1986).
- [25] CRC Handbook of Chemistry and Physics, 71st edition, (CRC Press, Boca Raton, 1990).